# Sequence-Dependent Peptide Binding Orientation by the Molecular Chaperone DnaK†

Tim L. Tapley, Jill R. Cupp-Vickery, and Larry E. Vickery*

*Department of Physiology and Biophysics, University of California, Irvine, California 92697*

*Received June 14, 2005; Revised Manuscript Received July 13, 2005*

ABSTRACT: Hsp70-class molecular chaperones interact with diverse polypeptide substrates, but there is limited information on the structures of different Hsp70−peptide complexes. We have used a site-directed fluorescence labeling and quenching strategy to investigate the orientation of different peptides bound to DnaK from *Escherichia coli*. DnaK was selectively labeled on opposite sides of the substrate-binding domain (SBD) with the fluorescent probe bimane, and the ability of peptides containing N- or C-terminal tryptophan residues to quench bimane fluorescence was measured. Tryptophan-labeled derivatives of the model peptide NRLLLTG bound with the same *forward* orientation previously observed in the crystal structure of the DnaK(SBD)−NRLLLTG complex. Derivatives of this peptide containing arginine in the C-terminal rather than N-terminal region, NTLLLRG, also bound in the forward direction indicating that charged residues in the flanking regions of the peptide are not the major determinant of peptide binding orientation. We also tested peptides having proline in one (ELPLVKI) or two (ELPPVKI) central positions. Tryptophan derivatives of each of these peptides bound with a strong preference for the *reverse* direction relative to that observed for the NRLLLTG and NTLLLRG peptides. Computer modeling the peptides NRLLLTG and ELPPVKI in both the forward and reverse orientations into the DnaK(SBD) indicated that differential hydrogen-bonding patterns and steric constraints of the central peptide residues are likely causes for differences in their binding orientations. These findings establish that DnaK is able to bind substrates in both forward and reverse orientations and suggest that the central residues of the peptide are the major determinants of directional preference.

Hsp70 molecular chaperones participate in a variety of protein folding events and interact with diverse polypeptide substrates (see refs *1*−*3* for reviews). There is limited information, however, on the structures of Hsp70 proteins in complex with different peptides. Crystallographic (*4*) and solution NMR (*5*) studies of the isolated substrate binding domain (SBD)[1] of DnaK complexed with the synthetic peptide NRLLLTG have revealed that the peptide is bound in an extended conformation in a hydrophobic cleft within the $\beta$-subdomain of the SBD. The specificity and stability of the complex appear to arise from nonpolar interactions involving side chains of the peptide and hydrogen-bonding interactions involving the main chain of the peptide and DnaK residues lining the binding cleft. Selectivity appears to be greatest at a central hydrophobic pocket designated cleft site "0", and the backbone and side chain of the central leucine residue bound in this position are completely enclosed by the chaperone (*4*, *5*). NMR studies on a fragment of the DnaK(SBD) without added peptide have also shown that an unfolded segment near the truncated C-terminus, $^{540}$DHLLHSTR$^{547}$, can bind in the cleft with Leu$^{543}$ held in the central hydrophobic pocket at cleft site 0 (*6*). In both the NRLLLTG peptide and DnaK "pseudosubstrate" complexes, the peptide is bound in a similar "front-to-back" (*forward*) orientation.

We have recently begun characterization of the interaction of peptide substrates with HscA, a specialized Hsp70 involved in the biogenesis of iron−sulfur proteins (*7*−*10*). HscA recognizes a specific LPPVK sequence motif of IscU, an Fe−S cluster scaffold protein, and synthetic peptides containing the LPPVK sequence interact with HscA in a manner similar to the IscU protein (*11*). Surprisingly, recent studies have revealed that the IscU protein and LPPVK-containing peptides bind to HscA in an orientation opposite that observed in the previously characterized DnaK(SBD)−peptide complexes. Fluorescence quenching studies using site-specifically labeled HscA, tryptophan-labeled IscU, and IscU-derived peptides showed that the LPPVK region binds to full-length HscA in a "back-to-front" (*reverse*) orientation (*12*). Subsequent X-ray crystallographic studies of a HscA(SBD)−ELPPVKIHC complex confirmed that the peptide is bound in the reverse orientation relative to DnaK(SBD)−peptide complexes and that the central proline residue of the peptide (Pro4) is bound at cleft site 0 (*13*). This structure also revealed differences in stereochemical constraints, hydrogen-bonding patterns, and electrostatic interactions in the peptide complex of HscA compared to that of DnaK. Differences in the peptide-binding clefts of HscA and DnaK and differences in the peptides studied, however, make it difficult to evaluate whether peptide-binding orientation is

† This work was supported by National Institutes of Health Grant GM54264.

* To whom correspondence should be addressed. Tel, (949) 824-6580; fax, (949) 824-8540; e-mail, lvickery@uci.edu.

[1] Abbreviations: SBD, substrate binding domain; rmsd, root-mean-square deviation. The abbreviations used for synthetic peptides are given in Table 1.

10.1021/bi051145r CCC: $30.25 
Published on Web 08/24/2005

determined by specific features of the chaperones or by properties of the peptide substrates.

In the studies described herein, we have employed a fluorescence-labeling and quenching strategy similar to that used previously with HscA to investigate peptide-binding orientation by DnaK. We have tested the possible role of charge location by moving the arginine residue of the NRLLLTG peptide from the N-terminal to the C-terminal flanking region (NTLLLRG). We have also studied the interaction of IscU-like peptides having centrally located proline residues (ELPPVKI and ELPLVKI) to determine whether changes in the structure of central residues affect directional binding preference.

## MATERIALS AND METHODS

*Synthetic Peptides.* Peptides (≥95% purity) were synthesized by the Protein and Nucleic Acid (PAN) Biotechnology facility at Stanford University, purified by high-pressure liquid chromatography, and analyzed by mass spectrometry. Peptide concentrations were determined gravimetrically and spectrophotometrically as previously described (*12*).

*Preparation of Bimane-Labeled DnaK.* The plasmid pJM2 (*14*) was used as a template for construction of DnaK mutants. The codon (TGT) for the single intrinsic cysteine ($Cys^{15}$) of DnaK was mutated to a serine codon (TCT) using the QuikChange technique (Stratagene). The plasmid incorporating the TGT → TCT substitution was then used as a template to introduce unique cysteine codons corresponding to residue positions 425 or 458, and mutations were confirmed by DNA sequencing (Laragen, Inc.). The double mutant proteins containing the $Cys^{15}$ → $Ser^{15}$ and $Val^{425}$ → $Cys^{425}$ or $Cys^{15}$ → $Ser^{15}$ and $Asn^{458}$ → $Cys^{458}$ were designated DnaK(V425C) and DnaK(N458C), respectively, and were expressed and purified as described previously for wild-type DnaK (*15*). Bimane labeling was carried out and quantified as described for HscA cysteine mutants (*12*). Labeling stoichiometries of 0.7−1.1 mol bimane/mol DnaK were obtained, consistent with specific labeling of the single cysteine residue.

*Steady-State Fluorescence Measurements.* Fluorescence measurements were recorded using a Cary Eclipse fluorescence spectrophotometer (Varian, Inc.). Samples contained 1 μM bimane-labeled DnaK(V425C) or DnaK(N458C) in 50 mM HEPES, 150 mM KCl, and 10 mM $MgCl_2$, pH 7.5 (HKM buffer), at 25 °C. For peptide binding titrations, samples contained 0.5 mM ATP to facilitate rapid peptide binding (*16*−*18*), and repetitive measurements were performed to verify equilibration. Emission spectra from 420 to 520 nm (10 nm band-pass) were recorded using an excitation wavelength of 395 nm (5 nm band-pass). Titrations were performed 2−3 times with similar results, and representative experiments are presented in Figures 2−6. Peptide concentrations are reported as the total peptide present, and binding constants reported are therefore apparent $K_d$ values. However, because titrations employed low concentrations of DnaK, the apparent values are close approximations to the dissociation constants. Because of the slow ATPase activity of DnaK and weak peptide stimulation, we estimate that less than 1% of the ATP present was hydrolyzed over the course of each titration (≤60 min; see Table 1 for rate constants).

*Measurement of ATP-Induced Peptide Release.* The nucleotide dependence of DnaK−peptide interactions was determined by monitoring fluorescence changes of bimane-labeled DnaK−peptide complexes in response to ATP binding. Peptide binding to nucleotide-free (*R*-state DnaK) is slow (*16*−*19*), and samples containing 1 μM DnaK(V425C)−bimane or DnaK(N458C)−bimane were incubated with 5−20 μM peptide for 1 h in the absence of nucleotide to allow peptide binding. Bimane fluorescence was monitored over time using an excitation wavelength of 395 nm (5 nm band-pass) and an emission wavelength of 475 nm (10 nm band-pass) with 2 s averaging. Fluorescence emission of preequilibrated samples was monitored for 100 s, at which point data acquisition was paused. Samples were treated with 10 μL of 10 mM ATP (100 μM final concentration) and mixed (∼10 s), and data acquisition was resumed.

Table 1: Sequences of Peptides and Their Tryptophan Derivatives[a]

| parent | N-terminal Trp | C-terminal Trp |
|---|---|---|
| NRLLLTG (NR) | W-NRLLLTG (W-NR) | NRLLLTG-W (NR-W) |
| NTLLLRG (NT) | W-NTLLLRG (W-NT) | NTLLLRG-W (NT-W) |
| ELPPVKI (PP) | W-ELPPVKI (W-PP) | ELPPVKI-W (PP-W) |
| ELPLVKI (PL) | W-ELPLVKI (W-PL) | ELPLVKI-W (PL-W) |

[a] Abbreviations used in the text are shown in parentheses.

*Peptide Modeling.* Models of peptides NRLLLTG (NR) and ELPPVKI (PP) bound to DnaK(SBD) in the forward and reverse orientations were constructed using the DnaK(SBD)−NRLLLTG cocrystal structure (PDB accession 1DKZ, (*4*)) as a template. Protein structures were aligned using CCP4 suite (*20*), and peptide structures were manually manipulated using FRODO (*21*). Energy minimizations of isolated and DnaK-bound peptides were performed using CNS (*22*). A detailed description of modeling methods and files containing the atomic coordinates of DnaK(SBD)−peptide model complexes are provided as Supporting Information.

*Other Methods.* Fluorescence emission spectra were corrected for dilution and integrated using Excel, and curve fitting was performed using Kaleidagraph (Synergy Software). ATPase assays were performed in triplicate at 25 °C using the EnzChek kit (Molecular Probes) and 25 μM DnaK in the absence or presence of peptide (50−200 μM) in HKM buffer supplemented with 0.5 mM ATP (*15*). Graphical representations of DnaK structures and DnaK−peptide models were generated using VMD (*23*).

## RESULTS AND DISCUSSION

*Experimental Rationale.* We have employed a site-specific fluorescence labeling and quenching strategy to assess the preferred peptide binding orientation of DnaK. This method takes advantage of quenching of the fluorescent probe bimane by tryptophan, a process that involves collisional contact between the bimane excited state and the indole ring of tryptophan (*24*). Bimane quenching has been used previously to examine short-range interactions in proteins and protein complexes (*25*), as well as to determine the preferred substrate-binding orientation of HscA (*12*).

To identify potential bimane labeling sites of DnaK that might selectively interact with N- or C-terminal residues of bound peptides, we examined the crystal structure of the DnaK(SBD)−NRLLLTG complex (*4*) for surface residues located near the flanking regions of the peptide-binding cleft. In the standard view shown in Figure 1, the N-terminus of

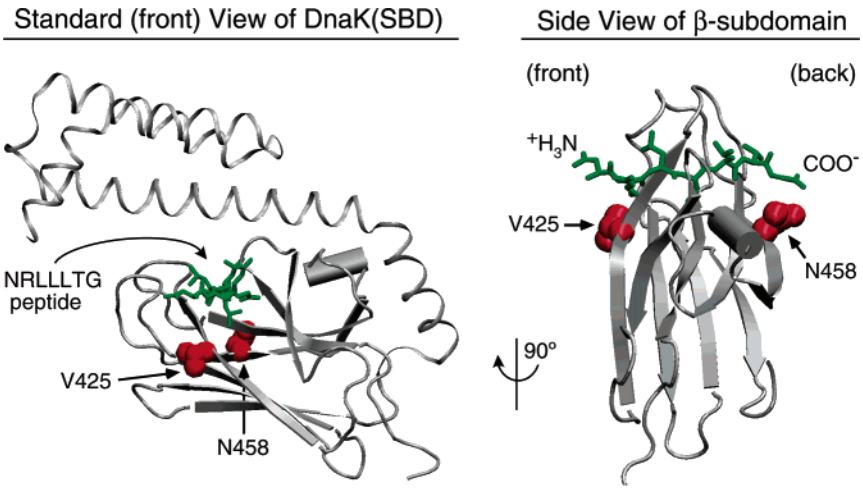


FIGURE 1: Structure of the DnaK(SBD)−NRLLLTG complex (adapted from ref *4*). The peptide backbone of DnaK is illustrated in cartoon form (gray), and the NR peptide is shown as a stick structure (green). Sites chosen for mutagenesis to cysteine ($Val^{425}$ and $Asn^{458}$) for bimane labeling are indicated as space filling models (red). The α-helical lid subdomain of the SBD (residues 508−607) has been omitted in the side view. Graphical representations were generated using VMD (*23*).

the peptide is closest to the viewer on the "front" side of the SBD and the C-terminus is on the "back" side. The side view of the $\beta$-subdomain shows that the N- and C-termini of the peptide lie at the ends of the cleft close to the protein surface. $Val^{425}$ and $Asn^{458}$ on the front and backsides of DnaK, respectively, are positioned close to the peptide termini and appeared to provide suitable sites for attachment of bimane labels for possible interaction with peptide derivatives having tryptophan at the N- or C-terminus.

Four sets of peptides and their derivatives were selected for study (Table 1). NRLLLTG (NR) was chosen because its orientation when bound to DnaK(SBD) has been well-established in the crystalline state by X-ray diffraction methods (*4*) and in solution by NMR methods (*5*). Derivatives of the NR peptide having tryptophan at the N- or C-terminus, designated W-NR and NR-W, respectively, were used for fluorescence-quenching studies. A related peptide, NTLLLRG (NT), in which the positions of the arginine and threonine residues of the NR peptide are interchanged, was chosen to assess the effect of charge distribution on binding orientation, and tryptophan derivatives of NT (W-NT and NT-W) were used for quenching studies. Two proline-containing peptides, ELPPVKI (PP) and ELPLVKI (PL), and their tryptophan derivatives were also chosen to assess possible effects of the central residues on directional binding preference. The PP peptide binds to HscA in the reverse orientation (*12*, *13*) and thus allows direct assessment of whether substrate-binding orientation is determined primarily by properties of the peptide substrate or by structural features of the chaperone. The PL peptide has a leucine residue in the central position similar to the NR and NT peptides and thus allows assessment of the relative importance of the central residues in determining binding orientation.

*Characterization of DnaK Mutants.* The single endogenous cysteine ($Cys^{15}$) of DnaK was replaced with serine, and $Val^{425}$ and $Asn^{458}$ were separately replaced with cysteine to generate the mutants DnaK(V425C) and DnaK(N458C) having unique bimane-labeling sites. Both mutants exhibited chromatographic behavior, far-UV CD spectra, and ATP-induced changes in intrinsic tryptophan fluorescence (*26*) very similar to that of wild-type DnaK (data not shown), indicating that there were no major structural changes as a result of the mutations introduced. $Cys^{15}$ is positioned close to the nucleotide-binding site in DnaK (*27*), and replacement of the homologous cysteine of bovine Hsc70 with lysine or arginine has been reported to reduce ATPase activity (*28*). To further assess possible effects of the Cys → Ser, Val → Cys, and Asn → Cys substitutions on the functional properties of the DnaK(V425C) and DnaK(N458C) mutants ,we measured intrinsic rates of ATP hydrolysis and stimulation by the NR, NT, PP, and PL peptides (Table 2). The basal ATPase activities of both DnaK(V425C) (0.015 $min^{-1}$) and DnaK(N458C) (0.010 $min^{-1}$) were reduced somewhat compared to that of wild-type DnaK (0.022 $min^{-1}$), and the observed decreases in catalytic activity may result from replacement of $Cys^{15}$ with serine and/or substitution of cysteine at positions 425 or 458. The ATPase activity of both mutants, however, was enhanced by each of the peptides to an extent consistent with previous studies (∼2−10-fold, see *1*, *2*, and references therein). The stimulation of DnaK(V425C) varied from 3.2- to 4.0-fold with different peptides and from 1.8- to 3.0-fold for DnaK(N458C). The values for DnaK(V425C) are similar to those observed with wild-type DnaK (2.6- to 3.9-fold), but the values for DnaK(N458C) are lower, an effect that may result from the lower affinity of this mutant for peptides (see Figures 3−6). The finding that the activity of both mutants was enhanced by each peptide, however, suggests that both forms retain allosteric activation and interact with these substrates in a manner similar to wild-type DnaK protein.

Table 2: Peptide Stimulation of DnaK ATPase Activity[a]

| | | fold stimulation | | | |
|---|---|---|---|---|---|
| | basal activity | +NR | +NT | +PP | +PL |
| wild-type DnaK | 0.022 ± 0.0005 $min^{-1}$ | 3.6 | 3.9 | 2.6 | 2.6 |
| DnaK(V425C) | 0.015 ± 0.0001 $min^{-1}$ | 3.6 | 4.0 | 3.4 | 3.2 |
| DnaK(N458C) | 0.010 ± 0.0001 $min^{-1}$ | 2.7 | 3.0 | 1.8 | 1.9 |

[a] Basal activity is expressed as (mol ATP hydrolyzed/mol DnaK)/min. Fold stimulation values correspond to the increase in activity elicited by addition of NR or NT peptide (50 $\mu$M final concentration) or PP or PL peptide (200 $\mu$M final concentration).

*Interactions with NRLLLTG Peptides.* The affinity of DnaK for peptide substrates and the kinetics of peptide binding and release are nucleotide-dependent, with nucle-

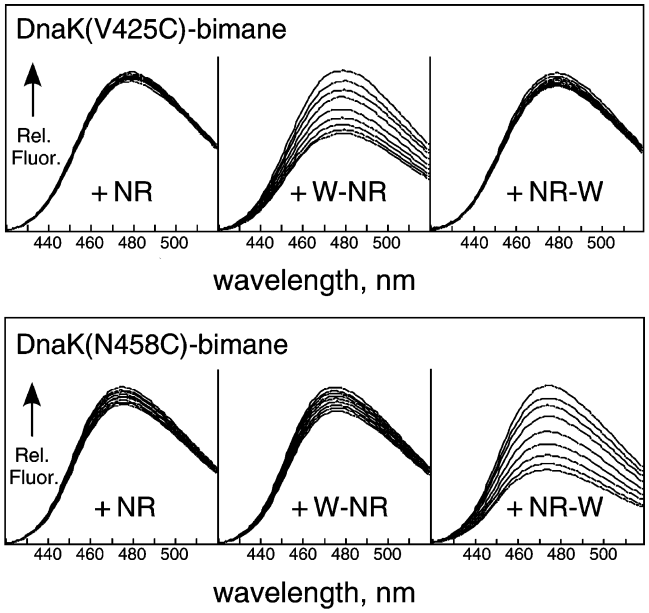


FIGURE 2: Effects of NRLLLTG (NR) peptides on the fluorescence of bimane-labeled DnaK. Emission spectra of samples in HKM buffer containing 0.5 mM ATP were recorded following successive additions of NR, W-NR, or NR-W (2−74 $\mu$M final concentrations). The uppermost spectrum for each sample was recorded prior to addition of peptide.

otide-free and ADP (R-state) complexes exhibiting higher substrate affinity and slower exchange rates than the DnaK·ATP (T-state) complex (*16*−*19*, *29*). As expected, on the basis of previous studies, bimane-labeled DnaK mutants in the absence of nucleotide exhibited very slow peptide-binding kinetics, with equilibration times up to 1 h (data not shown). For this reason, we performed all peptide titrations in the presence of ATP to facilitate rapid peptide binding. Emission spectra of bimane-labeled DnaK(V425C) and DnaK(N458C) in the presence of increasing concentrations of the NR, W-NR, and NR-W peptides are shown in Figure 2. The fluorescence of front side-labeled DnaK(V425C)−bimane was efficiently quenched by the W-NR peptide, whereas NR and NR-W caused only small changes in fluorescence intensity. The difference in quenching efficiency of the W-NR and NR-W peptides indicates that binding favors an orientation in which the N-terminus of the peptide is positioned close to residue 425 of DnaK on the front side of the SBD. Backside-labeled DnaK(N458C)−bimane, in contrast, was quenched most efficiently by the NR-W peptide, with NR and W-NR causing smaller decreases in fluorescence. This result indicates that the C-terminus of the bound peptides is close to residue 458 of DnaK on the backside of the SBD. The findings with both front- and backside-labeled DnaK are in agreement with the forward orientation of the NR peptide bound to DnaK(SBD) observed in the crystallographic (*4*) and solution NMR (*5*) studies. The finding that the NR peptide is bound in the same direction in the full-length DnaK derivatives studied here as was observed in the isolated DnaK(SBD) fragments suggests that directional binding preference is determined primarily by interactions within the SBD and is not affected by the ATPase domain. Furthermore, these findings indicate that neither introduction of the bimane label nor addition of tryptophan to the peptide termini results in an alteration of the preferred binding orientation of this peptide.

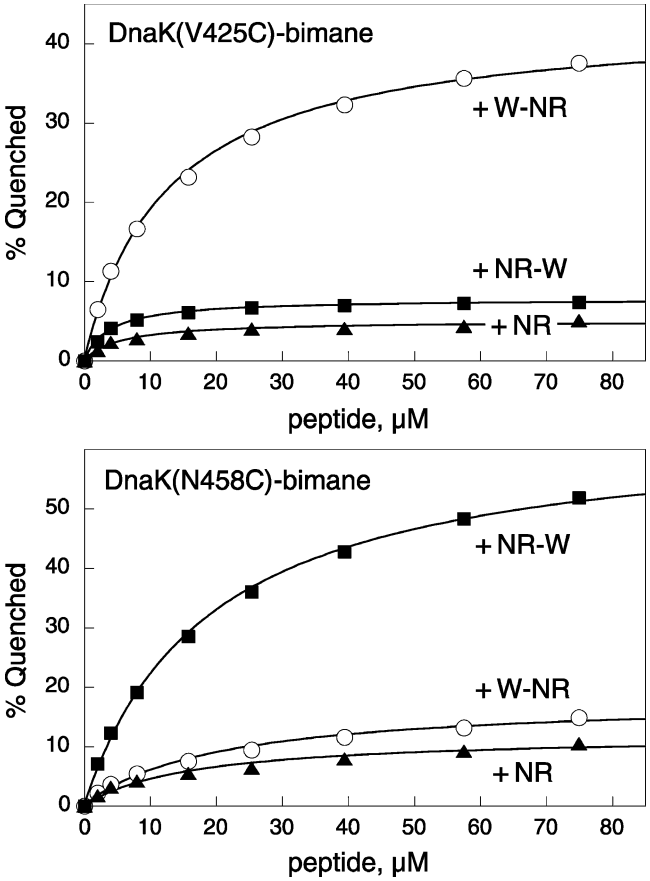


FIGURE 3: Binding of NRLLLTG (NR) peptides to bimane-labeled DnaK. Fractional quenching values determined from the integrated emission intensities in Figure 2 were plotted versus peptide concentration and fit to hyperbolic saturation functions to determine apparent $K_d$ and maximal quenching. DnaK(V425C)−bimane: +W-NR (○) $K_d^{app}$ = 13 $\mu$M (max = 43%); +NR-W (■) $K_d^{app}$ = 4 $\mu$M (max = 8%); +NR (▲) $K_d^{app}$ = 6 $\mu$M (max = 5%). DnaK(N458C)−bimane: +W-NR (○) $K_d^{app}$ = 20 $\mu$M (max = 18%); +NR-W (■) $K_d^{app}$ = 19 $\mu$M (max = 64%); +NR (▲) $K_d^{app}$ = 17 $\mu$M (max = 12%).

The binding affinity of the NR peptides for the DnaK−bimane derivatives and the maximal quenching values for each of the peptides were determined by plotting the integrated emissions shown in Figure 2 versus the concentration of added peptide (Figure 3). For bimane-labeled DnaK(V425C), all three NR peptides bound with similar affinity ($K_d^{app} \cong 4-13$ $\mu$M), indicating that the presence of tryptophan at the N- or C-terminus does not significantly alter binding interactions. For DnaK(N458C)−bimane, the affinities observed were slightly lower ($K_d^{app} \cong 17-20$ $\mu$M), and the bimane label attached at position 458 may be sufficiently close to the peptide cleft to cause some degree of interference with peptide binding. The binding affinities observed for both mutants are in general agreement with the previously published range of ≅25−85 $\mu$M for NR peptide derivatives binding to DnaK·ATP (*16*, *17*, *30*, *31*) consistent with the expected mode of binding. Comparison of the calculated maximal quenching values observed for the N- and C-terminal tryptophan derivatives indicates that ≥90% of the NR peptides were bound in the forward orientation for both the DnaK(V425C)−bimane and DnaK(N458C)−bimane forms.

*Effect of Charge Location on Peptide-Binding Orientation.* DnaK favors binding of peptides containing nonpolar

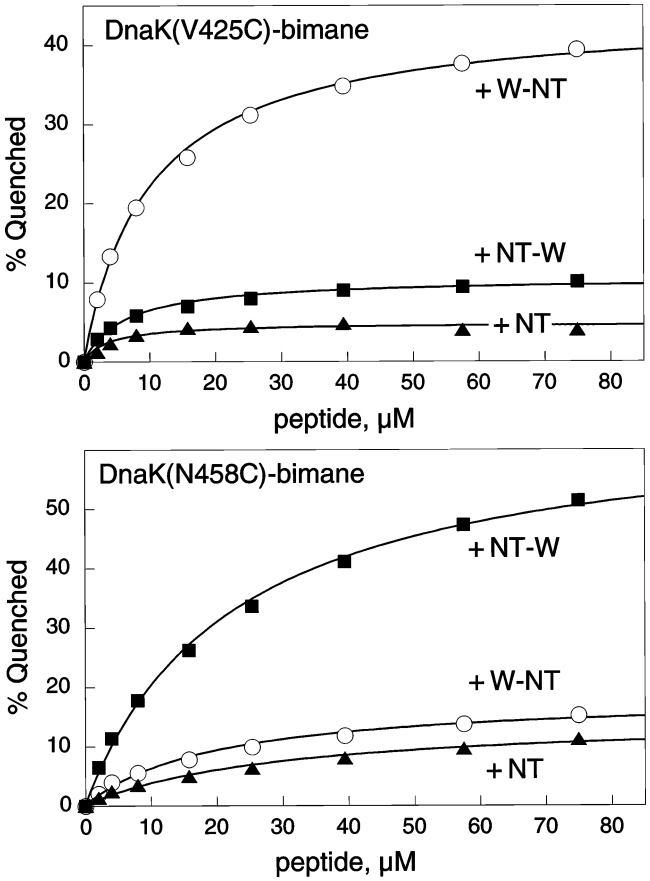


FIGURE 4: Binding of NTLLLRG (NT) peptides to bimane-labeled DnaK. Emission spectra were recorded and analyzed as in Figure 3 to determine apparent $K_d$ and maximal quenching. DnaK(V425C)−bimane: +W-NT (○) $K_d^{app}$ = 10 $\mu$M (max = 44%); +NT-W (■) $K_d^{app}$ = 6 $\mu$M (max = 10%); +NT (▲) $K_d^{app}$ = 4 $\mu$M (max = 5%). DnaK(N458C)−bimane: +W-NT (○) $K_d^{app}$ = 20 $\mu$M (max = 19%); +NT-W (■) $K_d^{app}$ = 23 $\mu$M (max = 66%); +NT (▲) $K_d^{app}$ = 30 $\mu$M (max = 15%).

residues in the central region flanked by basic residues (*32*, *33*). Consistent with these findings, the crystal structure of the DnaK(SBD)−NRLLLTG complex revealed that the central portion of the binding cleft is hydrophobic and that the nearby exterior regions have a negative electrostatic potential (*4*). However, the electronegative surface potential of the cleft region is greater on the backside where the negatively charged C-terminus of the peptide is located, and the positively charged arginine residue and N-terminus of the peptide are located on the less electronegative front side of the cleft. These observations suggest that electrostatic effects may not be important factors in determining binding orientation. To investigate possible effects of substrate charge distribution on binding direction, we studied the interaction of bimane-labeled DnaK with tryptophan derivatives of the NT peptide in which the basic arginine residue is located in the C-terminal flanking region rather than the N-terminal region as in the NR peptide. Titrations of DnaK(V425C)−bimane and DnaK(N458C)−bimane with NT, W-NT, and NT-W peptides were carried out as described for the NR peptides, and analyses of the integrated emission intensities versus peptide concentration are shown in Figure 4. The results are very similar to those obtained with the NR peptides (Figure 3); fluorescence of front side-labeled DnaK(V425C)−bimane was quenched most effectively by the N-terminal tryptophan derivative W-NT, and that of backside labeled DnaK(V458C)−bimane was quenched most effectively by the C-terminal tryptophan derivative NT-W. As with the NR peptides, the maximal quenching values observed suggest that ≥90% of NT peptides are bound in the forward orientation. The finding that the forward binding direction is strongly preferred whether arginine is located on the N- or C-terminal flanking region suggests that charge distribution within the peptide is not the major determinant of directional binding preference. In addition, the peptide-binding affinities observed (≅4−10 $\mu$M) for DnaK(V425C)−bimane and (≅20−30 $\mu$M) for DnaK(N458C)−bimane were very similar to those observed for NR peptides suggesting that charge location does not have a substantial effect on binding affinity. This is consistent with previous studies that found the peptide NRLLLRG to bind DnaK with higher affinity than NRLLLTG (*34*) and indicates arginine residues are capable of making favorable interactions with either side of the DnaK substrate binding domain.

*Interactions with Proline-Containing Peptides.* In contrast to the findings with the NR and NT peptides binding to DnaK, similar studies with HscA on the interaction of peptides containing the central recognition motif LPPVK showed that these peptides bind in a reverse, back-to-front, orientation (*12*). Crystallographic studies of a HscA(SBD)−ELPPVKIHC complex (*13*) confirmed this binding orientation and revealed that peptide residue Pro4 is bound in a hydrophobic pocket at cleft site 0 similar to peptide residue Leu4 in the DnaK(SBD)−NRLLLTG complex (*4*). The presence of proline residues and the reverse orientation of the peptide resulted in slight shifts in the peptide main- and side-chain positions as well as differences in hydrogen-bonding and electrostatic interactions between the peptide and the chaperone compared to that of the DnaK(SBD)−NRLLLTG complex.

To investigate the effect of the structure of the central-peptide residues on substrate-binding orientation, we characterized the interaction of bimane-labeled DnaK with two proline-containing peptides. We first tested derivatives of the peptide ELPPVKI (PP) found to bind in the reverse orientation to HscA. Figure 5 shows analyses of titrations of DnaK(V425C)−bimane and DnaK(N458C)−bimane with the PP, W-PP, and PP-W peptides. In contrast to findings with the NR and NT peptides, front side-labeled DnaK(V425C)−bimane was quenched most efficiently by the C-terminal tryptophan peptide (PP-W), and backside-labeled DnaK(N458C)−bimane was quenched most efficiently by the N-terminal tryptophan peptide (W-PP). These results are the opposite of those observed with the NR and NT peptides and indicate that PP peptides bind with an orientation reversed compared to that of NR and NT peptides. The difference in quenching efficiency between the N- and C-terminal tryptophan derivatives indicates a strong (≥90%) preference for the reverse binding direction for the PP peptides. The apparent binding affinities observed (∼20−200 $\mu$M), however, are somewhat lower than those observed for the NR and NT peptides. Binding of peptides containing acidic residues in the flanking regions to DnaK is moderately disfavored (*32*, *33*), and some of the decrease in affinity may be a result of unfavorable interactions between the negatively charged glutamate at the peptide N-terminus and the negative potential near the DnaK substrate-binding cleft. However,

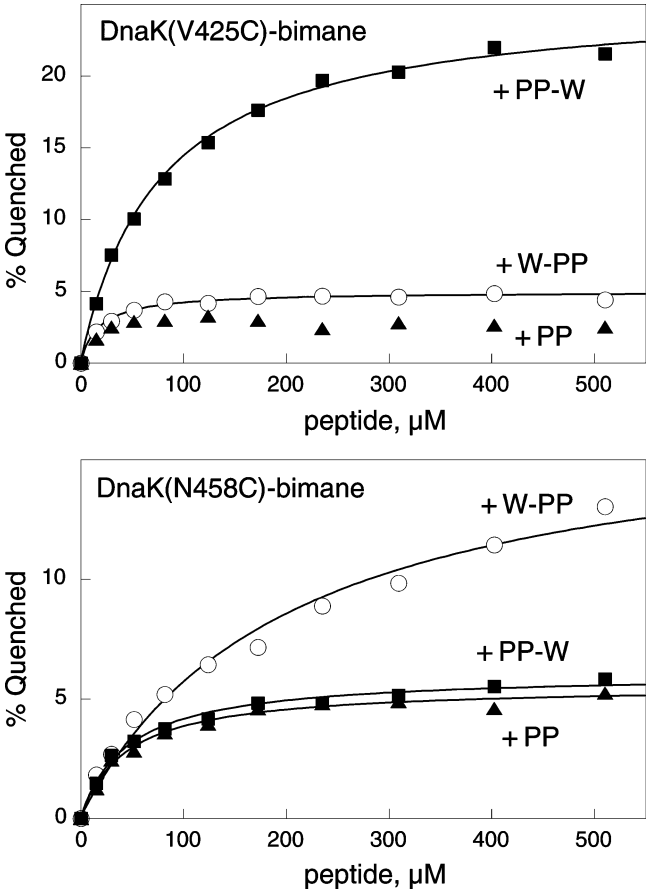


FIGURE 5: Binding of ELPPVKI (PP) peptides to bimane-labeled DnaK. Emission spectra were recorded and analyzed as in Figure 3 to determine apparent $K_d$ and maximal quenching. DnaK(V425C)−bimane: +W-PP (○) $K_d^{app} \sim 18$ $\mu$M (max = 5%); +PP-W (■) $K_d^{app} = 77$ $\mu$M (max = 26%); +PP (▲) not fit, max ~ 3%. DnaK(N458C)−bimane: +W-PP (○) $K_d^{app} = 200$ $\mu$M (max = 17%); +PP-W (■) $K_d^{app} = 45$ $\mu$M (max = 7%); +PP (▲) $K_d^{app} = 40$ $\mu$M (max = 6%).

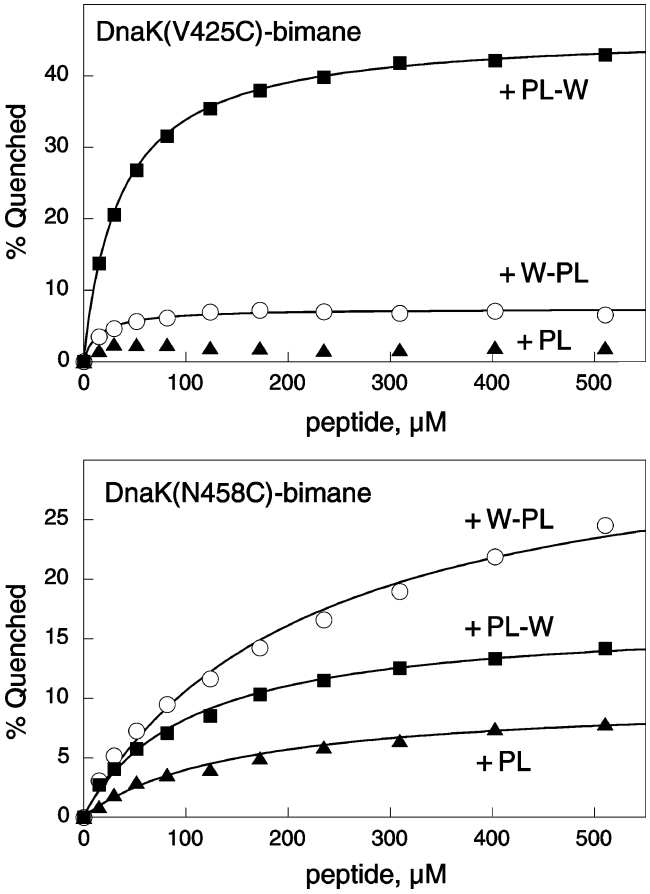


FIGURE 6: Binding of ELPLVKI (PL) peptides to bimane-labeled DnaK. Emission spectra were recorded and analyzed as in Figure 3 to determine apparent $K_d$ and maximal quenching. DnaK(V425C)−bimane: +W-PL (○) $K_d^{app} = 16$ $\mu$M (max = 7%); +PL-W (■) $K_d^{app} = 37$ $\mu$M (max = 46%); +PL (▲) not fit, max ~ 2%. DnaK(N458C)−bimane: +W-PL (○) $K_d^{app} = 260$ $\mu$M (max = 37%); +PL-W (■) $K_d^{app} = 105$ $\mu$M (max = 17%); +PL (▲) $K_d^{app} = 170$ $\mu$M (max = 11%).

it seems unlikely that Glu1 is the dominant factor determining peptide-binding orientation, because the pseudosubstrate DHLLHSTR contains an acidic residue in the corresponding position (Asp1) and binds DnaK in the forward orientation (*6*). Binding of proline-containing peptides to DnaK is disfavored compared to typical DnaK substrates (*32*, *33*), and stereochemical constraints imposed by the central proline residues of the PP peptides and/or loss of hydrogen bonds could affect the stability of the complex and alter the directional preference. The low affinity of DnaK(N458C)−bimane for the W-PP (and W-PL, see Figure 6) peptide suggests that unfavorable steric interactions between the bimane label and Trp side chains may occur when the peptide is bound in the reverse orientation, but these steric clashes do not appear to alter binding orientation.

To determine whether the reverse binding orientation observed with the PP peptides was due solely to the presence of proline in the central position, we tested similar peptides having a leucine residue at this location (PL, W-PL, and PL-W). Figure 6 shows analyses of titrations of DnaK(V425C)−bimane and DnaK(N458C)−bimane with these derivatives. As found for the PP peptides, front side-labeled DnaK(V425C)−bimane was quenched most efficiently by the C-terminal tryptophan labeled peptide (PL-W), and backside-labeled DnaK(N458C)−bimane was quenched most efficiently by the N-terminal tryptophan peptide (W-PL). Thus, the PL peptides, like the PP peptides, bind to DnaK with an orientation opposite that of the NR and NT peptides. The preference for the reverse binding direction, however, does not appear to be as great for the PL peptides as for the PP peptides, and some differences were observed in the degree of directional preference between the front and backside bimane-labeled forms of DnaK. For DnaK(V425C)−bimane, the PL-W, W-PL, and PL peptides gave calculated maximal quenching values of 46% versus 7% and ~2%, respectively, corresponding to ≅9:1 preference for the reverse orientation. For DnaK(N458C)−bimane, the PL-W, W-PL, and PL peptides gave calculated maximal quenching values of 17% versus 11% and 37%, respectively, corresponding to a somewhat less stringent (≅7.7:1) preference for the reverse orientation. As was observed with the W-PP peptide, DnaK(N458C)−bimane exhibited a decreased affinity for W-PL relative to the other two peptides, again raising the possibility of steric clashes between the bimane label and C- or N-terminal Trp residues. These unfavorable steric interactions only occur when the peptide is bound in the reverse orientation and may account for the small differences in directional preference observed between front- and backside-labeled DnaK.

The results with the PP and PL peptides establish that DnaK substrate-binding orientation is peptide sequence-dependent and suggest that proline residues in particular can result in an alteration in binding direction. The presence of a single proline near the central region appears sufficient to favor binding in the reverse orientation, and the occurrence of two adjacent proline residues strongly favors binding in the reverse orientation.

*Nucleotide Effects on Peptide Binding.* To determine whether bimane-labeled DnaK derivatives retain nucleotide-dependent allosteric regulation of substrate affinity and to determine whether the same peptide-binding orientation is observed in the R (nucleotide-free)- and T (ATP-bound)-states, we also measured peptide-induced quenching in the absence of ATP. The slow kinetics of substrate binding to R-state DnaK precluded titrations such as those carried out in the presence of ATP (Figures 2−6), and experiments were instead conducted using a single concentration of each peptide. Nucleotide-free DnaK−bimane derivatives were equilibrated with concentrations of peptide near or below the $K_d$ value for ATP-bound DnaK and were incubated for 1 h to allow peptide binding. Fluorescence emission was then monitored at 475 nm for 100 s prior to and following treatment with 100 $\mu$M ATP. Figure 7 presents results obtained using the NR and PP peptide derivatives. In each case, addition of ATP resulted in increased fluorescence (i.e., a reduction of peptide-mediated quenching), consistent with rapid release of the peptide substrate. The difference in peptide-binding affinity in the absence and presence of ATP is also apparent when comparing the extent of initial quenching by each of the peptides in Figure 7 (i.e., prior to ATP addition) with that observed at similar peptide concentrations in the titrations carried out in the presence of ATP (compare Figures 3 and 5). These results are consistent with the expected higher binding affinity of the peptides for the R-state (nucleotide-free) than for the T-state (ATP complex) and indicate that both DnaK(V425C)−bimane and DnaK(N458C)−bimane retain the allosteric interactions indicative of specific binding to the DnaK SBD.

The fluorescence emission intensities observed in Figure 7 prior to ATP addition also show that the NR and PP peptides exhibit the same preference for binding orientation to the R-state as observed for the T-state. For DnaK(V425C)−bimane, the W-NR peptide was more effective at quenching than the NR-W or NR peptides, consistent with positioning of the N-terminus of the bound peptide on the front side of the DnaK SBD, that is, the same forward orientation as was observed in the presence of ATP (Figures 2 and 3). In contrast, the PP-W peptide was a more effective quencher than the W-PP or PP peptides, consistent with positioning of the C-terminus of the bound peptide on the front side of the DnaK(SBD), that is, the reverse orientation as was observed in the presence of ATP (Figure 5). The results with the DnaK(458C)−bimane derivative yield the same conclusions. In this case, the NR-W and W-PP peptides were the most effective at quenching, as expected, for binding of the NR peptides in the forward direction and the PP peptides in the reverse direction. Similar experiments were also performed with the NT and PL peptides and both DnaK−bimane derivatives and yielded comparable results (rapid ATP-induced peptide release, binding of NT peptides in the forward direction, and binding of PL peptides in the reverse direction; data not shown). These findings indicate that for both forward- (NR and NT derivatives) and reverse-bound (PP and PL derivatives) peptides the preference for binding orientation is retained whether DnaK is in the R (nucleotide-free) or T (ATP complex) conformation.

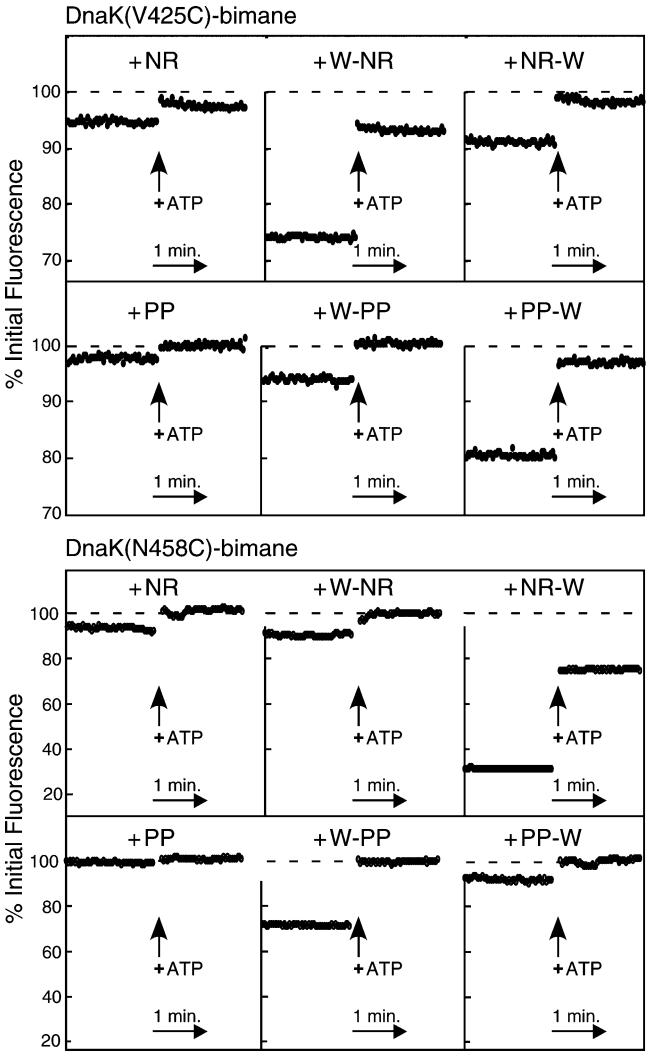


FIGURE 7: ATP-induced peptide release from bimane-labeled DnaK(V425C) and DnaK(N458C). Fluorescence emission of pre-equilibrated DnaK−peptide complexes (DnaK, 1 $\mu$M; W-NR, NR-W, or NR, 5 $\mu$M; W-PP, PP-W, or PP, 20 $\mu$M) was monitored at 475 nm for 100 s before and after addition of 100 $\mu$M ATP. The dashed lines (100%) indicate the level of fluorescence intensity prior to addition of peptide. Data have been corrected for the effects of ATP addition alone.

*Structural Basis of Peptide-Binding Orientation.* The results presented herein establish that DnaK can bind peptides in both the forward and reverse orientations and that the direction of peptide binding depends on the identity of the residues in the central region of the peptide. To gain insight into structural features of different DnaK−peptide complexes that might influence substrate binding orientation, we examined the structure of the DnaK(SBD)−NRLLLTG complex and modeled both the NR and PP peptides into DnaK(SBD) in both orientations. For interaction of the NR peptide with DnaK(SBD) in the forward orientation, no modeling was necessary, as this complex has been studied extensively by both X-ray crystallography (*4*) and solution NMR methods (*5*). When the NR peptide is bound in the forward orientation, the peptide backbone of the three central

leucine residues makes four hydrogen bonds to DnaK, resulting in all but two of the potential hydrogen bonds of the central residues being satisfied (see Supporting Information, Figure S1). Because of the hydrophobic nature of the binding pocket, these bonding interactions may constitute a significant energetic contribution to peptide binding, and previous studies have indicated that the hydrogen-bonding network in DnaK−peptide complexes may dictate substrate directionality (*35*).

A computer-generated model of DnaK complexed with the NR peptide in the reverse orientation was produced by manual rotation of the peptide in the binding pocket followed by energy minimization. Examination of the potential bonding interactions between the $NR_{reverse}$ peptide and DnaK reveals that the majority of peptide backbone hydrogen bonds are lost compared to the DnaK(SBD)−$NR_{forward}$ complex (see Supporting Information, Figure S1). In the reverse orientation, only two peptide backbone atoms are in position to form hydrogen bonds with the protein, resulting in four unsatisfied backbone hydrogen-bonding groups in the central three residues of the peptide. The DnaK(SBD)−$NR_{forward}$ and DnaK(SBD)−$NR_{reverse}$ complexes have similar hydrophobic contacts in the peptide binding cleft, and therefore, differences in backbone hydrogen-bonding interactions may be the key factors in determining directional preference.

Computer modeling with the PP peptide provided insight into the possible structural basis for the experimentally determined binding preference for this peptide as well. The DnaK(SBD)−$PP_{reverse}$ model was generated by superposition of the $\beta$-subdomains of DnaK and HscA and positioning the PP peptide from the HscA(SBD)−ELPPVKIHC structure (*13*) in the aligned DnaK protein followed by energy minimization. Two views of the DnaK(SBD)−PP complex are shown in Figure 8. In the reverse orientation, the peptide can be accommodated in the binding cleft without significant steric interference, and three of the four possible backbone hydrogen bonds between the central residues of the peptide and DnaK are satisfied. The side chain of Pro4 at the central position is smaller than the corresponding leucine residue found in the NR peptide, and this results in the peptide backbone being positioned somewhat lower in the binding cleft. For these reasons, the DnaK(SBD)−$PP_{reverse}$ complex has different bonding interactions from those seen in the DnaK(SBD)−$NR_{reverse}$ complex. The altered positioning of the peptide backbone due to the presence of proline residues and the ability to form hydrogen bonds may contribute to binding of the PP peptide in the reverse orientation, whereas the NR peptide binds in the forward orientation.

To examine how the PP peptide would fit in the peptide-binding cleft of DnaK in the forward orientation, we modeled the peptide using the DnaK(SBD)−$PP_{reverse}$ model as the initial template. To generate the DnaK(SBD)−$PP_{forward}$ model, the peptide was rotated 180° while maintaining the position of Pro4. Rotation of the peptide into the forward orientation resulted in significant steric interference between Pro3 and the protein backbone near residue Ser427 (Figure 8a). The B-factors (∼12−13) for the backbone atoms of Ser427 in the DnaK(SBD) crystal structure indicate low mobility in this region (*4*), suggesting that the protein backbone may not be able to move sufficiently to alleviate such interference. Energy minimization of the DnaK(SBD)−$PP_{forward}$ model in which Pro4 is fixed in the binding pocket

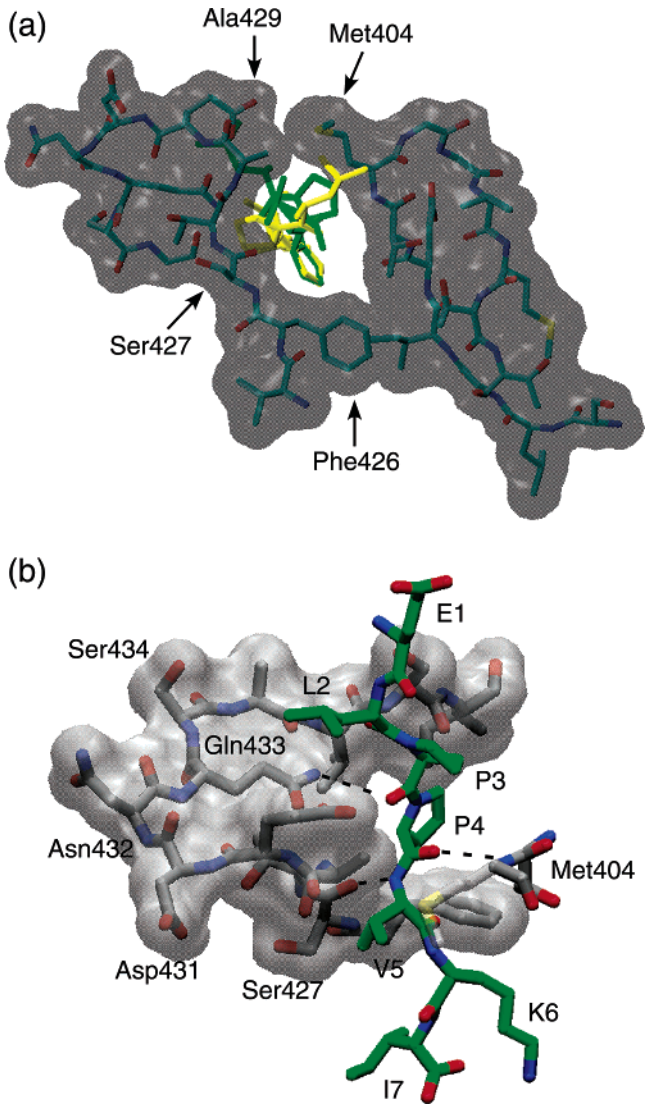


FIGURE 8: (a) Computer generated models of the peptide ELPPVKI (PP) bound to DnaK in the forward and reverse orientations. Residues 400−411 and 425−435 of DnaK(SBD) (*4*) are shown as both stick models (carbon, cyan; oxygen, red; nitrogen, blue; sulfur, yellow) and transparent space filling representations (gray). The peptide is modeled in forward (yellow) and reverse (green) orientations with the side chain of P4 superimposed in the central hydrophobic pocket of the binding cleft. (b) Computer generated model of the PP peptide bound to DnaK in the reverse orientation, with potential hydrogen bonds shown as dashed lines (coloring scheme is as in panel a with the exception that peptide carbon atoms are green). See text for discussion.

revealed that the steric clash of Pro3 and the protein backbone could not be avoided unless the $C_\alpha$ angles of the peptide are rotated to a high-energy conformation (rmsd of 1.8 Å compared to the energy minimized peptide). These results suggest that the geometrical restrictions of the proline residues located in the central region of the peptide restrict the peptide conformation to one that allows only the reverse orientation as observed in the HscA(SBD)−peptide structure (*13*).

*Summary.* The findings presented herein establish that DnaK is able to bind substrates in both forward and reverse orientations, and the modeling studies suggest that differences in hydrogen-bonding patterns and steric constraints imposed by central residues of bound peptides are key determinants of directional preference. The ability of DnaK to accom-

modate peptides with different sequences by binding them in opposite orientations could serve to broaden the substrate repertoire of DnaK and thereby enhance its role as a general stress response chaperone. Binding of peptides in forward and reverse orientations could also have important functional consequences for other Hsp70 chaperones, and subsets of polypeptide substrates may bind in a specific orientation as required for participation of the chaperone in a particular cellular process. Studies on the interaction of additional peptide sequences with other Hsp70s will be required to elucidate the rules governing substrate recognition and binding orientation.

## ACKNOWLEDGMENT

We thank Dennis Ta for expert technical assistance.

## SUPPORTING INFORMATION AVAILABLE

Detailed modeling methods, model complexes of DnaK(SBD) with NR peptide bound in forward and reverse orientations (Figure S1), PDB files containing atomic coordinates of DnaK−peptide model complexes. This material is available free of charge via the Internet at http://pubs.acs.org.

## REFERENCES

1. Mayer, M. P., and Bukau, B. (1998) Hsp70 chaperone systems: diversity of cellular functions and mechanism of action, *Biol. Chem. 379*, 261−268.
2. Mayer, M. P., Brehmer, D., Gassler, C. S., and Bukau, B. (2001) Hsp70 chaperone machines, *Adv. Protein Chem. 59*, 1−44.
3. Mayer, M. P., and Bukau, B. (2005) Hsp70 chaperones: cellular functions and molecular mechanism, *Cell. Mol. Life Sci. 62*, 670−684.
4. Zhu, X., Zhao, X., Burkholder, W. F., Gragerov, A., Ogata, C. M., Gottesman, M. E., and Hendrickson, W. A. (1996) Structural analysis of substrate binding by the molecular chaperone DnaK, *Science 272*, 1606−1614.
5. Stevens, S. Y., Cai, S., Pellecchia, M., and Zuiderweg, E. R. (2003) The solution structure of the bacterial HSP70 chaperone protein domain DnaK(393-507) in complex with the peptide NRLLLTG, *Protein Sci. 12*, 2588−2596.
6. Wang, H., Kurochkin, A. V., Pang, Y., Hu, W., Flynn, G. C., and Zuiderweg, E. R. (1998) NMR solution structure of the 21 kDa chaperone protein DnaK substrate binding domain: a preview of chaperone−protein interaction, *Biochemistry 37*, 7929−7940.
7. Strain, J., Lorenz, C. R., Bode, J., Garland, S., Smolen, G. A., Ta, D. T., Vickery, L. E., and Culotta, V. C. (1998) Suppressors of superoxide dismutase (SOD1) deficiency in *Saccharomyces cerevisiae*. Identification of proteins predicted to mediate iron−sulfur cluster assembly, *J. Biol. Chem. 273*, 31138−31144.
8. Zheng, L., Cash, V. L., Flint, D. H., and Dean, D. R. (1998) Assembly of iron−sulfur clusters. Identification of an iscSUA-hscBA-dx gene cluster from *Azotobacter vinelandii*, *J. Biol. Chem. 273*, 13264−13272.
9. Takahashi, Y., and Nakamura, M. (1999) Functional assignment of the ORF2-iscS-iscU-iscA-hscB-hscA-fdx-ORF3 gene cluster involved in the assembly of Fe−S clusters in *Escherichia coli*, *J. Biochem. (Tokyo) 126*, 917−926.
10. Tokumoto, U., and Takahashi, Y. (2001) Genetic analysis of the isc operon in *Escherichia coli* involved in the biogenesis of cellular iron−sulfur protein, *J. Biochem. (Tokyo) 130*, 63−71.
11. Hoff, K. G., Ta, D. T., Tapley, T. L., Silberg, J. J., and Vickery, L. E. (2002) Hsc66 substrate specificity is directed toward a discrete region of the iron−sulfur cluster template protein IscU, *J. Biol. Chem. 277*, 27353−27359.
12. Tapley, T. L., and Vickery, L. E. (2004) Preferential substrate binding orientation by the molecular chaperone HscA, *J. Biol. Chem. 279*, 28435−28442.
13. Cupp-Vickery, J. R., Peterson, J. C., Ta, D. T., and Vickery, L. E. (2004) Crystal structure of the molecular chaperone HscA substrate binding domain complexed with the IscU recognition peptide ELPPVKIHC, *J. Mol. Biol. 342*, 1265−1278.
14. McCarty, J. S., and Walker, G. C. (1991) DnaK as a thermometer: threonine-199 is site of autophosphorylation and is critical for ATPase activity, *Proc. Natl. Acad. Sci. U.S.A. 88*, 9513−9517.
15. Vickery, L. E., Silberg, J. J., and Ta, D. T. (1997) Hsc66 and Hsc20, a new heat shock cognate molecular chaperone system from *Escherichia coli*, *Protein Sci. 6*, 1047−1056.
16. Pierpaoli, E. V., Gisler, S. M., and Christen, P. (1998) Sequence-specific rates of interaction of target peptides with the molecular chaperones DnaK and DnaJ, *Biochemistry 37*, 16741−16748.
17. Gisler, S. M., Pierpaoli, E. V., and Christen, P. (1998) Catapult mechanism renders the chaperone action of Hsp70 unidirectional, *J. Mol. Biol. 279*, 833−840.
18. Schmid, D., Baici, A., Gehring, H., and Christen, P. (1994) Kinetics of molecular chaperone action., *Science 263*, 971−973.
19. Pierpaoli, E. V., Sandmeier, E., Baici, A., Schonfeld, H. J., Gisler, S., and Christen, P. (1997) The power stroke of the DnaK/DnaJ/GrpE molecular chaperone system, *J. Mol. Biol. 269*, 757−768.
20. Collaborative Computational Project, Number 4. (1994) The CCP4 suite: programs for protein crystallography, *Acta Crystallogr., Sect. D 50*, 760−763.
21. Jones, T. A. (1985) Diffraction methods for biological macromolecules. Interactive computer graphics: FRODO, *Methods Enzymol. 115*, 157−171.
22. Brunger, A. T., Adams, P. D., Clore, G. M., DeLano, W. L., Gros, P., Grosse-Kunstleve, R. W., Jiang, J. S., Kuszewski, J., Nilges, M., Pannu, N. S., Read, R. J., Rice, L. M., Simonson, T., and Warren, G. L. (1998) Crystallography & NMR system: a new software suite for macromolecular structure determination, *Acta Crystallogr., Sect. D 54*, 905−921.
23. Humphrey, W., Dalke, A., and Schulten, K. (1996) vmd−visual molecular dynamics, *J. Mol. Graphics 14*, 33−38.
24. Sato, E., Sakashita, M., Kanaoka, Y., and Kosower, E. M. (1988) Novel fluorogenic substrates for microdetermination of chymotrypsin and aminopeptidases: bimane fluorescence appears after hydrolysis, *Bioorg. Chem. 16*, 298−306.
25. Mansoor, S. E., McHaourab, H. S., and Farrens, D. L. (2002) Mapping proximity within proteins using fluorescence spectroscopy. A study of T4 lysozyme showing that tryptophan residues quench bimane fluorescence, *Biochemistry 41*, 2475−2484.
26. Banecki, B., Zylicz, M., Bertoli, E., and Tanfani, F. (1992) Structural and functional relationships in DnaK and DnaK756 heat-shock proteins from *Escherichia coli*, *J. Biol. Chem. 267*, 25051−25058.
27. Harrison, C. J., Hayer-Hartl, M., Di Liberto, M., Hartl, F., and Kuriyan, J. (1997) Crystal structure of the nucleotide exchange factor GrpE bound to the ATPase domain of the molecular chaperone DnaK, *Science 276*, 431−435.
28. Wilbanks, S. M., and McKay, D. B. (1998) Structural replacement of active site monovalent cations by the epsilon-amino group of lysine in the ATPase fragment of bovine Hsc70, *Biochemistry 37*, 7456−7462.
29. McCarty, J. S., Buchberger, A., Reinstein, J., and Bukau, B. (1995) The role of ATP in the functional cycle of the DnaK chaperone system, *J. Mol. Biol. 249*, 126−137.
30. Han, W., and Christen, P. (2003) Interdomain communication in the molecular chaperone DnaK, *Biochem. J. 369*, 627−634.
31. Slepenkov, S. V., and Witt, S. N. (2002) Kinetic analysis of interdomain coupling in a lidless variant of the molecular chaperone DnaK: DnaK's lid inhibits transition to the low affinity state, *Biochemistry 41*, 12224−12235.
32. Rudiger, S., Germeroth, L., Schneider-Mergener, J., and Bukau, B. (1997) Substrate specificity of the DnaK chaperone determined by screening cellulose-bound peptide libraries, *EMBO J. 16*, 1501−1507.
33. Gragerov, A., Zeng, L., Zhao, X., Burkholder, W., and Gottesman, M. E. (1994) Specificity of DnaK−peptide binding, *J. Mol. Biol. 235*, 848−854.
34. Kasper, P., Christen, P., and Gehring, H. (2000) Empirical calculation of the relative free energies of peptide binding to the molecular chaperone DnaK, *Proteins 40*, 185−192.
35. Rudiger, S., Schneider-Mergener, J., and Bukau, B. (2001) Its substrate specificity characterizes the DnaJ co-chaperone as a scanning factor for the DnaK chaperone, *EMBO J. 20*, 1042−1050.

BI051145R